Space-charge divergence of an intense, unneutralized rectangular ion beam

Douglas A. Brown and John F. O'Hanlon
Department of Electrical and Computer Engineering, University of Arizona, Tucson, Arizona 85721
(Received 30 November 1992)

Space-charge effects are explored theoretically as an intense (beam current density $\gtrsim 1$ mA/cm^2), positively charged ion beam emerges from an aperture displaying a well-defined aspect ratio and enters into an electron-free region of space. In the absence of space-charge neutralization, the beam diverges under the influence of the mutual Coulomb repulsion of the ions. Under the assumption of a collisionless beam, the mass, the energy, and the phase-space density are conserved to generate a single, three-dimensional partial differential equation. This equation is then combined with Poisson's equation and solved analytically to provide the beam ion density and potential at any point in space. Applying the resulting expression to beams of varying energies and current densities, it is found that irrespective of the initial aspect ratio, intense beams of all energies and currents continuously diverge and ultimately relax into near-Gaussian profiles.

PACS number(s): 41.75.−i

I. INTRODUCTION

The ever increasing use of medium- to high-current ($I_b \gtrsim 1$ mA) ion beams in the microelectronics industry has elevated the importance of developing a rigorous understanding of the fundamental principles of beam formation, neutralization, and propagation. Recent theoretical and experimental work has demonstrated that intense ion beams, such as those used in ion implantation during semiconductor processing, are capable of entrapping and transporting particulate contamination over long distances [1–3]. Should transported particles reach the target wafer, a loss of yield may result. A thorough understanding of the mechanisms by which a space-charge-neutralized beam maintains a steady-state charge distribution is essential if the beam's ability to entrap particles is to be eliminated or reduced. However, before a neutralized beam can be fully analyzed, the initial charge density of the unneutralized beam must be known. Previous studies have postulated *a priori* a beam of Gaussian cross section [4–7]. However, theoretical justification for this assumption has remained absent from the literature.

Figure 1 displays a schematic representation of the beam under consideration. As shown, the beam system is comprised of four distinct segments: the *plasma source, drift region, beam plasma,* and the *sheath* at the beam-target interface. The beam itself is comprised of positive, nonrelativistic ions extracted continuously from the source, and provides a steady current to the target.

Ions in the source are extracted and accelerated by the large potential difference between the source and the beam line. Electrons emerging with the beam are reflected back into the source plasma by the electron suppression electrode, which also serves to confine neutralizing electrons to the beam plasma and maintain an electron-free drift region. Passing through this electrode, the ions are shaped into a narrow charge configuration of nearly uniform density and well-defined aspect ratio. Upon entering the drift region, the beam begins to expand as the ions respond to their mutual Coulomb repulsion.

In this work, the beam is studied as it emerges from the source and propagates through the drift region. The physics of the expanding beam is explored. Charge densities and potentials are calculated. In the drift region, the cross-sectional profile of the unneutralized beam is found as a function of position relative to the emission aperture. No *a priori* assumptions are made regarding the charge density or potential; however, the chamber enclosing the beam is taken to be rectangular. Energy, mass, phase-space volume, and electric flux (Poisson's equation) are all conserved to find self-consistent analytic expressions for the potential and space-charge density.

In the subsequent calculations, the initial ion density is assumed to be uniform across the electron suppression aperture. However, the techniques developed here apply equally well to arbitrary initial charge distributions. Upon conclusion of the analysis, it is found that irrespective of the initial aspect ratio, intense beams of all energies and currents eventually relax into similar, near-Gaussian profiles.

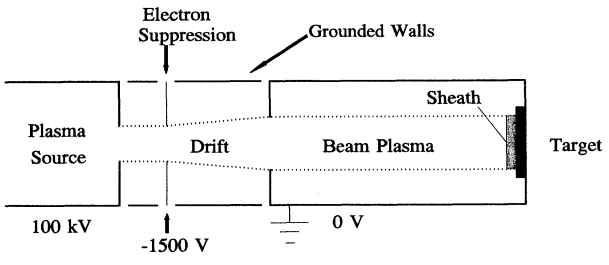

FIG. 1. Schematic illustration of the beam under study. Positively charged ions are extracted from the source, which is maintained at a high potential (~50–500 kV) with respect to the grounded beam line. In the drift region, the beam expands due to the ions' mutual Coulomb repulsion. Expansion is arrested in the beam line by screening effects of the plasma electrons.

II. THE DRIFTING, COLLISIONLESS BEAM

Properly designed extraction systems accelerate ions from the plasma source, launching them through the aperture in the electron suppression electrode and into the drift region with a nearly uniform cross-sectional density profile. Near the entrance to the drift region, the density has its largest value, typically on the order of $10^{14}-10^{18}$ m^{-3}. At these densities, the mean free path for hard collisions (contact scattering) is $\gtrsim 100$ m. Within the ion distribution, the potential of the ensemble varies, but is typically on the order of 1–100 V. Comparing spatial variations in the beam potential to the electric field of a two-particle Coulomb interaction, it is found that two ions would need to be less than 1 nm apart before the single-particle force approached that of the collective field. Therefore, it is reasonable to assume that scattering effects are negligible and that the trajectory of an individual ion is in direct response to a time constant, but spatially varying collective electric field.

Figure 2 depicts the situation to be studied. Ions emerge from an aperture of height h and width w located in the plane $z=0$. At this point, the density is assumed uniform; however, as the ions traverse the drift region, the beam broadens and the density is diminished, causing the potential to vary along the z as well as the x and y axes. The collective potential of the ensemble is defined to be zero at the origin, (0,0,0), and reaches its minimum relative value at the grounded conducting walls of a rectangular chamber.

Space-charge effects become important when the ion density is sufficiently large such that the expansion due to electrostatic forces is comparable to the thermal expansion of the beam. To obtain an estimate of the minimum ion density required to induce significant space-charge expansion, consider a uniform cylindrical beam of radius a and density n_{b0}, comprised of singly charged positive ions of mass m_b. In the plasma source, these ions possess a temperature, T (eV), that will be assumed to characterize the ions throughout the expanding beam. If q is the elementary unit of charge and U_e is the extraction potential, the ions will display a transverse thermal velocity, $v_{\rm th}=\sqrt{2qT/m_b}$ and a longitudinal velocity $v_b=\sqrt{2qU_e/m_b}$. Given velocities in m/s, the characteristic time for the beam to propagate 1 m is $t=\sqrt{m_b/2qU_e}$. During this time, the thermally induced radial expansion of the beam is on the order of $v_{\rm th}t=\sqrt{T/U_e}$. For a 10-eV source and a 100-keV beam, this corresponds to a characteristic expansion length, $d_{\rm th}=1$ cm.

From Gauss's law, the electric field external to the charge distribution is $E(r)=qn_{b0}a^2/2\epsilon_0 r$. An ion along the periphery of the beam experiences an acceleration

$$\ddot{r}=\frac{q^2n_{b0}a^2}{2\epsilon_0 m_b r} . \tag{1}$$

Since it is of interest to obtain an estimate of n_{b0} when the Coulomb expansion is comparable to the thermal expansion, it is permissible to employ the approximation $r\cong v_{\rm th}t$, which is correct within a prefactor of order unity for this restricted case. Equation (1) may then be integrated to yield

$$r\cong v_{\rm th}t+\frac{q^2n_{b0}a^2}{2\epsilon_0 m_b}\frac{t}{v_{\rm th}}(\ln t-1)+a . \tag{2}$$

For beam ions ranging in mass from 1–100 amu (1.66×10^{-27}–1.66×10^{-25} kg), with energies ranging between 10 and 100 keV, the characteristic propagation time is on the order of $t\sim10^{-6}$ s. Using this value of t, and setting $r=v_{\rm th}t$, it is found that the minimum density for significant space-charge effects scales as

$$n_{b0}\approx\frac{10^{10}}{a} , \tag{3}$$

where the density is per cubic meter, and a is in meters.

Thus a 2-cm-diam cylindrical ion beam will begin to display significant space-charge expansion when $n_{b0}\sim10^{12}$ m^{-3}. For ions with a beam velocity $v_b\sim10^6$ m/s, this volume density corresponds to a current density $J_b\sim20\ \mu$A/cm^2.

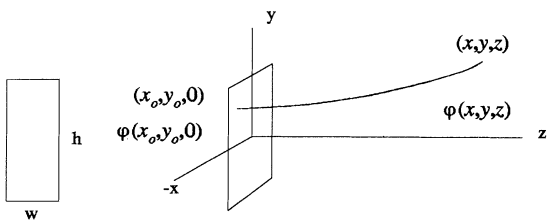

FIG. 2. Ions emerging from an aperture of width w and height h follow well-defined, energy-conserving trajectories. The potential is defined to be zero at the origin and attains its minimum at the walls of a rectangular chamber.

III. ENERGY CONSERVATION

In the limit of a collisionless beam, each ion can be assumed to travel a well-defined, deterministic trajectory. Thus, an unknown but physically determined trajectory is assumed. Following this single-particle trajectory (Fig. 2), an ion emerges from the aperture at some point $(x_0,y_0,0)$, and arrives sometime later at the point (x,y,z). The change in the kinetic energy of an ion with mass m_b, and charge q, is related to the potential by

$$\tfrac{1}{2}m_b[(\mathbf{v}+\Delta\mathbf{v})^2-\mathbf{v}^2]=-q[\phi(x,y,z)-\phi(x_0,y_0,0)] . \tag{4}$$

Expanding the velocity products and canceling terms, Eq. (4) becomes

$$\tfrac{1}{2}[(\Delta v_x)^2+(\Delta v_y)^2+(\Delta v_z)^2+2v_{x0}\Delta v_x+2v_{y0}\Delta v_y+2v_{z0}\Delta v_z]=-\frac{q}{m_b}[\phi(x,y,z)-\phi(x_0,y_0,0)] . \quad (5)$$

Formally, the change in velocity, $\Delta\mathbf{v}$, is the time integral of the acceleration. However, the time of flight is neither known, nor of interest. Therefore, the time shall be expressed in terms of the axial position, parametrized through the z component of velocity. Noting that, for a conservative field, the acceleration is proportional to the gradient of the potential, and setting $dt=dz/v_z$, the changes in velocity along each coordinate axis are given by

$$\Delta v_x=\frac{q}{m_b}\int_0^z\left[-\frac{\partial\phi}{\partial x}\right]\frac{dz}{v_z} , \quad \Delta v_y=\frac{q}{m_b}\int_0^z\left[-\frac{\partial\phi}{\partial y}\right]\frac{dz}{v_z} , \quad \Delta v_z=\frac{q}{m_b}\int_0^z\left[-\frac{\partial\phi}{\partial z}\right]\frac{dz}{v_z} .$$

Thus the energy conservation relation becomes

$$\frac{1}{2}\left[\left[\frac{q}{m_b}\int_0^z\left[-\frac{\partial\phi}{\partial x}\right]\frac{dz}{v_z}\right]^2+\left[\frac{q}{m_b}\int_0^z\left[-\frac{\partial\phi}{\partial y}\right]\frac{dz}{v_z}\right]^2+\left[\frac{q}{m_b}\int_0^z\left[-\frac{\partial\phi}{\partial z}\right]\frac{dz}{v_z}\right]^2+2v_{x0}\frac{q}{m_b}\int_0^z\left[-\frac{\partial\phi}{\partial x}\right]\frac{dz}{v_z}\right.$$
$$\left.+2v_{y0}\frac{q}{m_b}\int_0^z\left[-\frac{\partial\phi}{\partial y}\right]\frac{dz}{v_z}+2v_{z0}\frac{q}{m_b}\int_0^z\left[-\frac{\partial\phi}{\partial z}\right]\frac{dz}{v_z}\right]=-\frac{q}{m_b}[\phi(x,y,z)-\phi(x_0,y_0,0)] . \quad (6)$$

Equation (6) is a nonlinear integral relation. It can, however, be brought into tractable form by partially differentiating with respect to z. Care must be exercised when differentiating the right-hand side. In the development of Eq. (6), a deterministic trajectory was assumed. When the expression is partially differentiated along the z axis, x and y are held fixed. The trajectory then determines the initial point $(x_0,y_0,0)$. In this way, x_0 and y_0 are not constants, but rather are functions of z. Differentiation thus yields

$$v_{x0}\frac{\partial\phi}{\partial x}-\frac{\partial\phi}{\partial x}\int_0^z\frac{q}{m_b}\left[\frac{\partial\phi}{\partial x}\right]\frac{dz}{v_z}+v_{y0}\frac{\partial\phi}{\partial y}-\frac{\partial\phi}{\partial y}\int_0^z\frac{q}{m_b}\left[\frac{\partial\phi}{\partial y}\right]\frac{dz}{v_z}+v_{z0}\frac{\partial\phi}{\partial z}-\frac{\partial\phi}{\partial z}\int_0^z\frac{q}{m_b}\left[\frac{\partial\phi}{\partial z}\right]\frac{dz}{v_z}$$
$$=v_z\left[\frac{\partial\phi}{\partial z}-\frac{\partial\phi}{\partial x_0}\frac{\partial x_0}{\partial z}-\frac{\partial\phi}{\partial y_0}\frac{\partial y_0}{\partial z}\right] . \quad (7)$$

Recognizing the left-hand side as the inner product of the velocity and the gradient of the potential, conservation of energy can be expressed in the compact form:

$$\mathbf{v}\cdot\nabla\phi(x,y,z)=v_z\left[\frac{\partial\phi}{\partial z}-\frac{\partial\phi}{\partial x_0}\frac{\partial x_0}{\partial z}-\frac{\partial\phi}{\partial y_0}\frac{\partial y_0}{\partial z}\right] . \quad (8)$$

IV. CONSERVATION OF PHASE-SPACE DENSITY

Classically, the equation governing the time-dependent phase-space evolution of a particle system is the Boltzmann equation [8]

$$\frac{\partial f}{\partial t}+\mathbf{v}\cdot\nabla_{\mathbf{x}}f+\frac{1}{m_b}\mathbf{F}\cdot\nabla_{\mathbf{v}}f=\sum_{i=1}^{N}(\xi_i^+-\xi_i^-) , \quad (9)$$

where $f=f(\mathbf{x},\mathbf{v},t)$ is the distribution function, N is the total number of particles in the ensemble, t is the time, $\mathbf{F}$ is a conservative force acting on particles at $\mathbf{x}$, and $(\mathbf{x},\mathbf{v})$ are the phase-space coordinates. The quantities ξ_i^+ and ξ_i^- are, respectively, the rates at which collisions send particles into or out of a given phase-space volume. In thermal equilibrium, or in a collisionless gas, these last two quantities are equal and the right-hand side of Eq. (9) vanishes.

As discussed in Sec. II, the ions' mean free path is large and the dimension for scattering small; thus, to a very good approximation, the beam is collisionless. Setting the right-hand side to zero, and expressing the force $\mathbf{F}$ in terms of the collective electric field of the ions, phase-space density conservation for the beam is expressed by the requirement

$$\frac{\partial f}{\partial t}+\mathbf{v}\cdot\nabla_{\mathbf{x}}f-\frac{q}{m_b}\nabla\phi\cdot\nabla_{\mathbf{v}}f=0 . \quad (10)$$

A stationary solution to Eq. (10) is the well-known Maxwell-Boltzmann distribution function. For a system of particles with mass m, at temperature T, this distribution is given by

$$f(\mathbf{x},\mathbf{v})=n(x,y,z)e^{-(m/2kT)\mathbf{v}\cdot\mathbf{v}} ,$$

where n is the number density of the ensemble and k is the Boltzmann constant.

However, the situation in the beam is not truly time independent, nor is the distribution stationary. An observer in the x-y plane traveling with the beam along the z axis will witness a time-varying particle density. Moreover, in the laboratory frame, conditions of thermal equilibrium clearly do not prevail and the concept of a temperature, T, becomes somewhat nebulous. To circumvent these difficulties, two observations are made. First, during expansion in the drift region, no external fields act against the motion of the ions, and the ions do no work. Therefore, in the absence of collisions with other particle species (e.g., residual gas molecules) there is no mechanism for cooling and the width of the Gaussian velocity distribution, $\sqrt{kT/m_b}$, does not change. Further, if the extraction field is assumed to accelerate each ion uniformly in the z direction, there is no heating in the ex-

traction gap prior to the drift region, and the beam temperature can be taken to be the temperature of the ions in the source plasma. (The condition of no heating will be rigorously true along the axis, but may lose some validity near the ensemble's periphery during extraction.) Second, if the shape of the velocity-space distribution function is constant, then the observer moving with the beam will detect a state of thermal quasiequilibrium characterized by a time-varying density of particles with a kinetic energy shifted by the beam velocity, $(m_b/2)[v_x^2+v_y^2+(v_z-v_b)^2]$, where v_z is the beam velocity in the laboratory reference frame and v_b is the velocity added during extraction from the source. In view of these arguments, a shifted Maxwellian velocity distribution can be assumed,

$$f(\mathbf{x},\mathbf{v},t)=n_b(\mathbf{x},t)e^{-(m_b/2kT)[v_x^2+v_y^2+(v_z-v_b)^2]} . \quad (11)$$

This is the distribution function in the beam's reference frame. The velocity distribution is stationary, but the particle density varies in time. To translate this function back into the laboratory frame, the time t is again parametrized in terms of the axial position z. Applying the chain rule to the time derivative of f, the first term of Eq. (10) can be written as

$$\frac{\partial f}{\partial t}=\frac{\partial f}{\partial z}\frac{\partial z}{\partial t}=v_z\frac{\partial f}{\partial z} .$$

Employing Eq. (11), and denoting the shifted velocity by $\mathbf{v}'=\mathbf{v}-v_b\mathbf{e}_z$, phase-space density conservation may be expressed as

$$v_z\frac{\partial n_b}{\partial z}+\mathbf{v}'\cdot\nabla n_b+\frac{q}{kT}\nabla\phi\cdot n_b\mathbf{v}'=0 .$$

The coefficients of the partial derivative of n_b with respect to z can be combined,

$$v_z\frac{\partial n_b}{\partial z}+(v_z-v_b)\frac{\partial n_b}{\partial z}=(2v_z-v_b)\frac{\partial n_b}{\partial z} .$$

Now, v_z is the sum of the extraction and thermal velocities. In any practical ion beam, the extraction velocity, v_b, is orders of magnitude greater than the thermal velocity in the plasma source. So, to a very good level of approximation, it is possible to write $2v_z-v_b\approx v_z$ (because $v_z\approx v_b+\delta$, $|\delta/v_b|\ll 1$), and conservation of phase-space density can be represented as

$$-\frac{1}{n_b}\mathbf{v}\cdot\nabla n_b=\frac{q}{kT}\mathbf{v}'\cdot\nabla\phi . \quad (12)$$

V. CONSERVATION OF MASS

In a collisionless beam, there is no random-scattering diffusion, and no creation or annihilation of particles. Mass conservation is thus characterized by the vanishing divergence of the particle current,

$$\nabla\cdot(n_b\mathbf{v})=0 .$$

Expanding this equation, it is possible to relate the divergence of the velocity to the gradient of the density,

$$\nabla\cdot\mathbf{v}=-\frac{1}{n_b}\mathbf{v}\cdot\nabla n_b . \quad (13)$$

VI. DERIVATION OF THE DRIFT EQUATION

Again parametrizing the time t in terms of z, the conservation laws of the preceding sections may be combined into a single homogeneous partial differential equation.

From Eqs. (12) and (13), the divergence of the velocity is related to the gradient of the potential by

$$\nabla\cdot\mathbf{v}=\frac{q}{kT}\mathbf{v}'\cdot\nabla\phi . \quad (14)$$

Recalling that $\mathbf{v}'=\mathbf{v}-v_b\mathbf{e}_z$, the right-hand side of this last expression may be written as

$$\frac{q}{kT}\mathbf{v}'\cdot\nabla\phi=\frac{q}{kT}\left[\mathbf{v}\cdot\nabla\phi-v_b\frac{\partial\phi}{\partial z}\right] .$$

Thus, the energy-conserving relation, Eq. (8), can be combined with (14) to yield

$$\nabla\cdot\mathbf{v}=\frac{q}{kT}\left[(v_z-v_b)\frac{\partial\phi}{\partial z}-v_z\left[\frac{\partial\phi}{\partial x_0}\frac{\partial x_0}{\partial z}+\frac{\partial\phi}{\partial y_0}\frac{\partial y_0}{\partial z}\right]\right] . \quad (15)$$

Parametrizing the time in terms of the z coordinate, the velocity is related to the potential through the integral relations:

$$\begin{aligned} v_x&=v_{x0}-\int_0^z\frac{q}{m_b}\frac{\partial\phi}{\partial x}\frac{dz}{v_z} ,\\ v_y&=v_{y0}-\int_0^z\frac{q}{m_b}\frac{\partial\phi}{\partial y}\frac{dz}{v_z} ,\\ v_z&=v_{z0}-\int_0^z\frac{q}{m_b}\frac{\partial\phi}{\partial z}\frac{dz}{v_z} . \end{aligned} \quad (16)$$

Thus the divergence of the velocity can also be written in terms of the potential,

$$\nabla\cdot\mathbf{v}=-\int_0^z\frac{q}{m_b}\frac{\partial^2\phi}{\partial x^2}\frac{dz}{v_z}-\int_0^z\frac{q}{m_b}\frac{\partial^2\phi}{\partial y^2}\frac{dz}{v_z}-\frac{q}{m_b}\frac{\partial\phi}{\partial z} . \quad (17)$$

With this result, Eq. (15) can be fully expressed in terms of the potential and the z component of velocity. Recall that the terms in Eq. (15) containing x_0 and y_0 are evaluated in the plane $z=0$. Then, noting that v_z varies weakly along the z axis, so that $\partial v_z/\partial z\approx 0$, substituting Eq. (17) into Eq. (15) and partially differentiating with respect to z produces

$$-\frac{q}{m_b v_z}\nabla^2\phi=\frac{q}{kT}\left[(v_z-v_b)\frac{\partial^2\phi}{\partial z^2}-v_z\left[\frac{\partial^2\phi}{\partial x_0^2}\frac{\partial x_0}{\partial z}+\frac{\partial^2\phi}{\partial y_0\partial x_0}\frac{\partial y_0}{\partial z}\right]\frac{\partial x_0}{\partial z}\right.$$
$$\left.-v_z\left[\frac{\partial^2\phi}{\partial x_0\partial y_0}\frac{\partial x_0}{\partial z}+\frac{\partial^2\phi}{\partial y_0^2}\frac{\partial y_0}{\partial z}\right]\frac{\partial y_0}{\partial z}-v_z\frac{\partial\phi}{\partial x_0}\frac{\partial^2 x_0}{\partial z^2}-v_z\frac{\partial\phi}{\partial y_0}\frac{\partial^2 y_0}{\partial z^2}\right]. \quad (18)$$

Equation (18) can be simplified by analyzing the derivatives. It is expected that ions along the periphery of the beam will experience the largest acceleration and display the trajectories of greatest curvature. Near the plane $z=0$, components of the electric field along the beam's periphery are essentially uniform. The ions' velocities increase at an approximately linear rate, and the time scales as $t\sim z/v_z$. The transverse position varies roughly as $(z/v_z)^2$. A typical beam velocities, the contribution from terms containing $(z/v_z)^2$ will be small relative to a peripheral ion's transverse coordinate and the ion trajectory will therefore possess very little curvature. Restated, in the region about which x_0 and y_0 are computed, the ion trajectories of greatest curvature are anticipated to be nearly linear. Consequently, the initial positions, $x_0(z)$ and $y_0(z)$, do not vary strongly with z, and, in particular, display little curvature; so $|\partial^2 x_0/\partial z^2|\sim|\partial^2 y_0/\partial z^2|\approx 0$. Moreover, the aperture and total beam divergence are small compared to the characteristic length of the beam (~ 1 m); so, the initial points can display only a weak linear dependence on z, and the terms involving products of derivatives, $v_z(\partial x_0/\partial z)^2\sim v_z(\partial y_0/\partial z)^2\sim v_z(\partial x_0/\partial z)(\partial y_0/\partial z)\ll(v_z-v_b)$, are also negligible. Thus, Eq. (18) is reducible to

$$\nabla^2\phi=-\frac{m_b}{kT}v_z(v_z-v_b)\frac{\partial^2\phi}{\partial z^2}\ . \quad (19)$$

As stated earlier, the quantity (v_z-v_b) is simply the z component of the thermal velocity possessed by the ion when it was in the source. After extraction, (v_z-v_b) is always positive; for a particle accelerated by a conservative field to an ultimate velocity with a component that is parallel to, and in the same direction as, the acting force cannot possess a kinetic energy less than the accelerating potential. That is, if qU_e is the extraction energy, then the minimum longitudinal velocity of a beam ion is $v_b=\sqrt{2qU_e/m_b}$. Taking the value of the thermal velocity to be the most probable velocity of the Maxwell-Boltzmann distribution, $\sqrt{2kT/m_b}$, and rearranging terms, Eq. (19) becomes

$$\frac{\partial^2\phi}{\partial x^2}+\frac{\partial^2\phi}{\partial y^2}+\left[1+v_z\left[\frac{2m_b}{kT}\right]^{1/2}\right]\frac{\partial^2\phi}{\partial z^2}=0\ .$$

Observing that the quantity in parentheses is never less than unity, it is permissible to define a new parameter, $\eta^2=(1+v_z\sqrt{2m_b/kT})>0$. The equation to be solved thereby assumes a simple form:

$$\frac{\partial^2\phi}{\partial x^2}+\frac{\partial^2\phi}{\partial y^2}+\eta^2\frac{\partial^2\phi}{\partial z^2}=0\ . \quad (20)$$

Equation (20) is the drift equation. It incorporates energy, mass, and phase-space density conservation to describe the expansion of a collisionless positive ion beam in an electron-free region of space.

VII. SOLUTION TO THE DRIFT EQUATION

Equation (20) is solvable by the method of separation of variables. For a rectangular chamber, two classes of solution emerge: sinusoids and exponentials. The appropriate choice of functions within each class derives from the geometric symmetry of the beam. Boundary conditions for the potential then impose requirements on the combinations of functions utilized in the construction of the final solution.

Clearly, the density must have similar functional dependence in both the x and y directions, and must display even parity with respect to these coordinates. The ion concentration must also possess a smooth, well-defined maximum at any point along the beam's axis. A cusp in the particle density would not represent a physical situation. Exponential functions cannot satisfy these criteria; so, the solution in the x-y plane is a combination of sinusoids. Of this class of solution, parity considerations demand the use of cosines, and preclude the appearance of the sine function.

Equation (20) is a three-dimensional elliptic partial

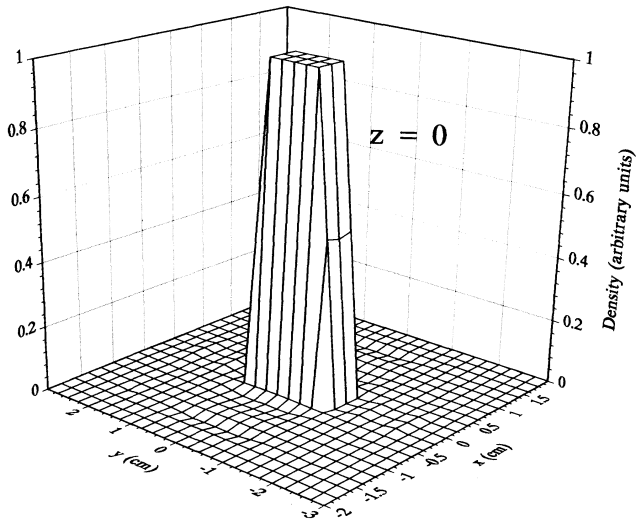

FIG. 3. Uniform density profile in the plane $z=0$. Due to the energy independence of the distribution in this plane, this profile applies to all beams emerging from an aperture 1.5 cm high and 0.5 cm wide.

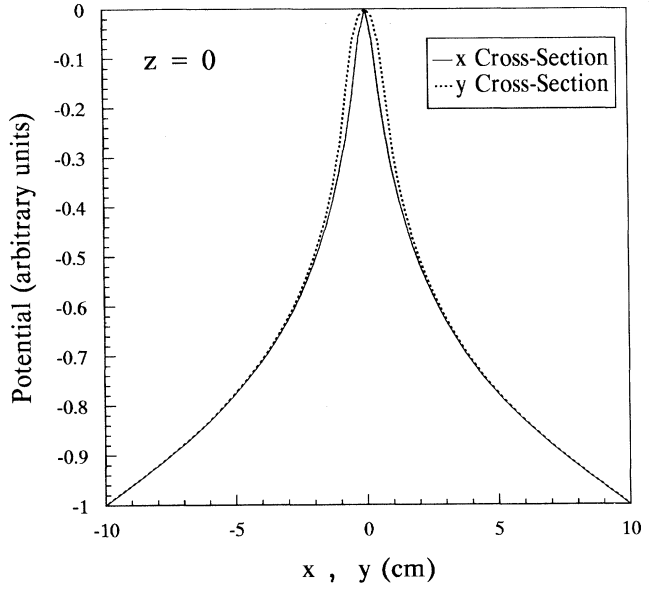

FIG. 4. Cross section of the potential at $z=0$ for the 3:1 aperture of Fig. 3. The potential across the y axis follows the uppermost curve, with the x-axis potential lying just underneath.

differential equation; thus, the selection of two sinusoidal functions in the x and y directions forces the solution in z to be exponential. Since no particles are created outside the source, the axial density cannot increase, and the ion concentation along the beam's axis must decay exponentially with increasing z.

In fulfilling these physical requirements, the solution to Eq. (20) becomes an exponentially decaying two-dimensional Fourier series:

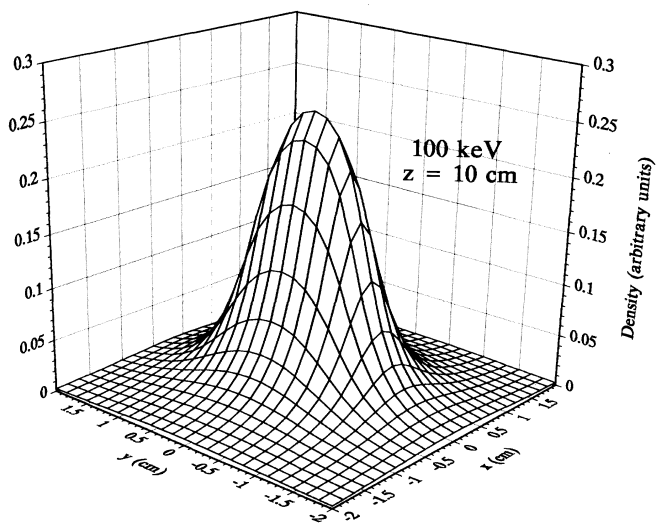

FIG. 5. At 10 cm from a 1.5×0.5 cm^2 emission aperture, a 100-keV beam displays significant broadening, but still retains a recognizable aspect ratio.

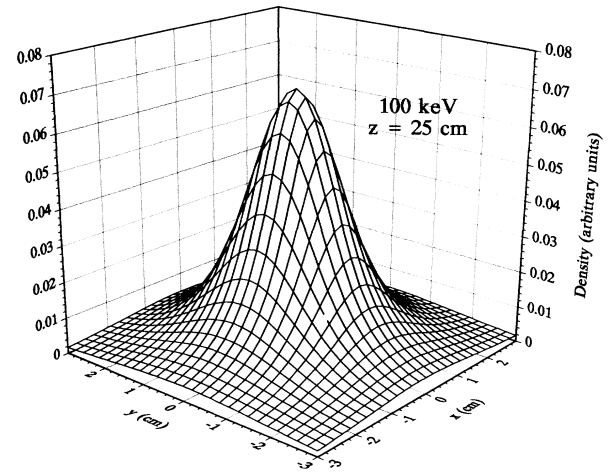

FIG. 6. At $z=25$ cm, the 100-keV beam of Fig. 3 has relaxed into a highly symmetric profile.

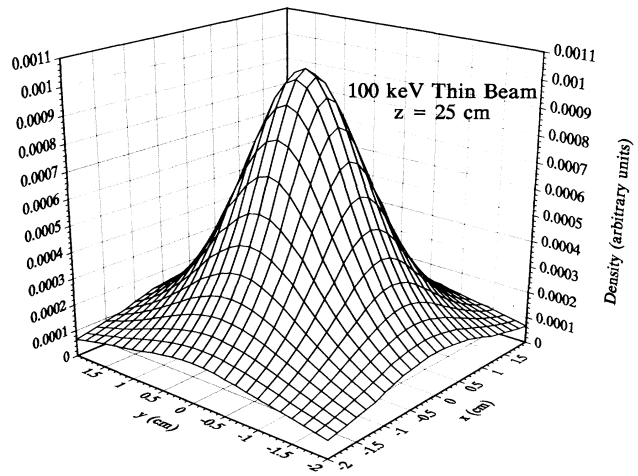

FIG. 7. Initial aspect ratios do not affect the ultimate beam shape. At 25 cm, a thin beam with an initial aspect ratio of 10:1 (1.0 cm$\times$0.1 cm) has assumed a shape essentially identical to beams originating from wider, shorter apertures.

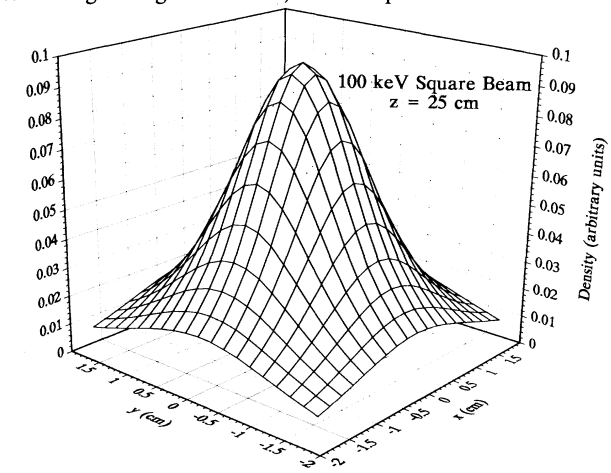

FIG. 8. An initially square beam presents a shape indistinguishable from that of an initially thin beam. The magnitude of the axial density is, however, considerably higher as much less ion movement is required for a square beam to attain this shape.

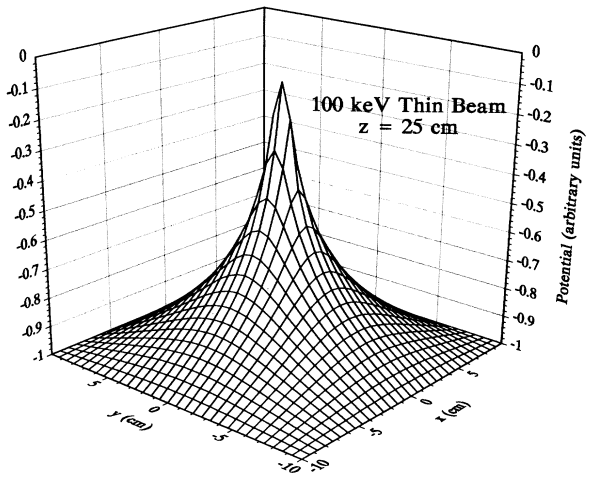

FIG. 9. Potential at $z=25$ cm for a 100-keV beam with an initial 10:1 aspect ratio. (1.0 cm$\times$0.1 cm).

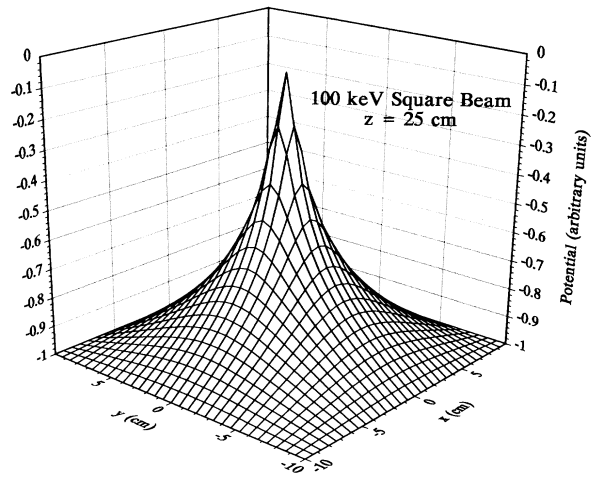

FIG. 10. Potential at $z=25$ cm for a 100-keV beam with an initial 1:1 aspect ratio.

$$\phi(x,y,z)=-\phi_0+\sum_{m,n=0}^{\infty} a_{mn}\cos(\alpha_n x)\cos(\beta_m y)e^{-(\gamma nm/\eta)z},$$
$$\alpha_n=\frac{(2n+1)\pi}{2L_x},$$
$$\beta_m=\frac{(2m+1)\pi}{2L_y}, \tag{21}$$
$$\gamma_{nm}=\frac{\pi}{2}\left[\left[\frac{2n+1}{L_x}\right]^2+\left[\frac{2m+1}{L_y}\right]^2\right]^{1/2},$$

where ϕ_0 is the value of the sum at the origin, and L_x and L_y are the distances along each coordinate axis from the center of the beam to the conducting wall. The coefficients α_n and β_m are constructed such that the series vanishes at the chamber wall, thereby enforcing the boundary requirement of constant potential.

The solution is constrained by the requirement that the potential satisfy Poisson's equation, which in Système International units is given by

$$\nabla^2\phi(x,y,z)=-\frac{q}{\epsilon_0}n(x,y,z).$$

From Eq. (20), the Laplacian of the potential can be expressed in terms of the second partial derivative with respect to z,

$$\nabla^2\phi(x,y,z)=(1-\eta^2)\frac{\partial^2\phi}{\partial z^2}.$$

Using the solution for ϕ [Eq. (21)], and combining this last result with Poisson's equation yields the following expression for the density:

$$n(x,y,z)=\left[1-\frac{1}{\eta^2}\right]\frac{\epsilon_0}{q}\sum_{m,n=0}^{\infty} a_{mn}\gamma_{nm}^2\cos(\alpha_n x)\cos(\beta_m y)e^{-(\gamma nm/\eta)z}. \tag{22}$$

Assuming an initially uniform density, the ion density in the plane $z=0$ is n_{b0} when $|x|\le w/2$ and $|y|\le h/2$, and zero elsewhere. Evaluation of the coefficients, a_{mn}, over this region is straightforward, and yields

$$a_{mn}=n_{b0}\frac{q}{\epsilon_0}\frac{64}{\pi^4}\frac{\sin\left[\beta_m\frac{h}{2}\right]\sin\left[\alpha_n\frac{w}{2}\right]}{(2n+1)(2m+1)\left[\left[\frac{2n+1}{L_x}\right]^2+\left[\frac{2m+1}{L_y}\right]^2\right]}. \tag{23}$$

Equations (21) and (22) with coefficients (23) completely describe the density and potential of the positive ion distribution at every point in the drift region.

VIII. DENSITIES AND POTENTIALS IN THE DRIFT REGION

Equations (21) and (22) were evaluated for 50-, 100-, and 500-keV ion beams. It was found that each of these beams ultimately relaxed into a near-Gaussian profile, with the higher-energy beams relaxing after traversing greater longitudinal distances. This latter behavior arises from the energy dependence of η in the exponential term. With $v_z\cong v_b=\sqrt{2qU_e/m_b}$, the defining relation for η becomes $\eta\cong(1+2\sqrt{qU_e/kT})^{1/2}$. Thus, at higher beam energies, γ_{nm}/η becomes smaller and z must be larger to induce the same density profile. The altering of the basic

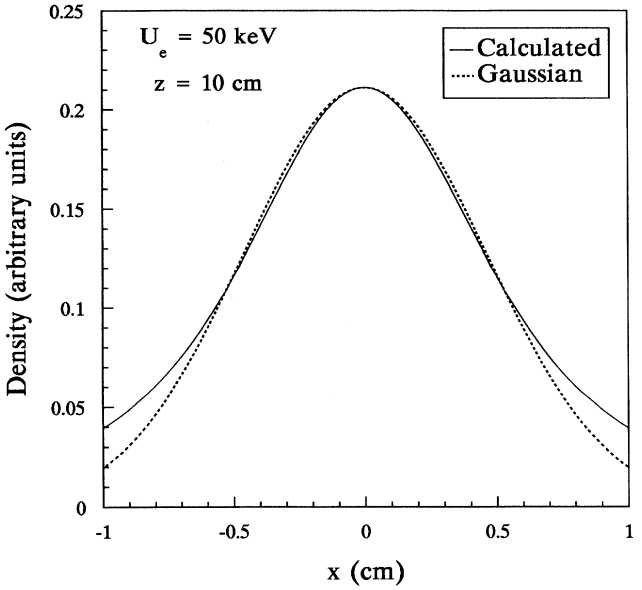

FIG. 11. The 50-keV beam, 10 cm from the emission aperture. Curve-fitting a Gaussian along a single coordinate axis produces very good agreement between the points of half maximum.

beam shape to a profile of greater symmetry is anticipated, as the system is expected to evolve into a configuration of minimum potential energy.

In the figures, the densities and potentials have been normalized to unity at the origin of coordinates. Relative volumes confined by the three-dimensional density surfaces are constant, and the number of particles conserved.

Figure 3 displays the uniform density at the entrance to the drift region. The aperture has a height of 1.5 cm,

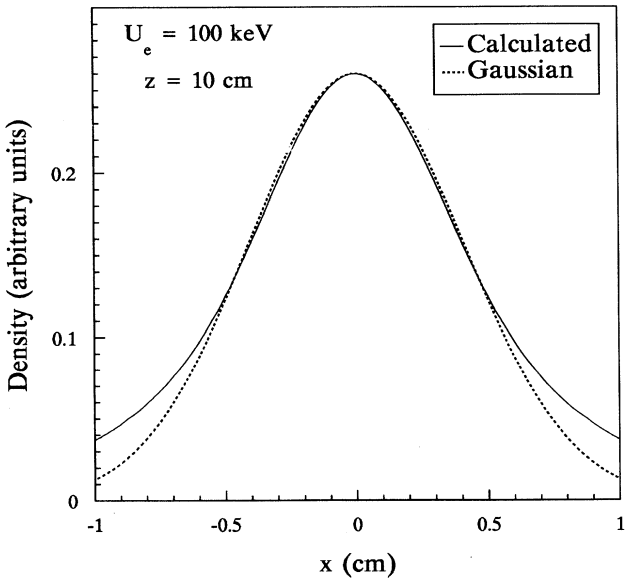

FIG. 12. The 100-keV beam, 10 cm from the emission aperture. Even at twice the energy, the Gaussian curve provides a good fit in the region about the maximum of the distribution.

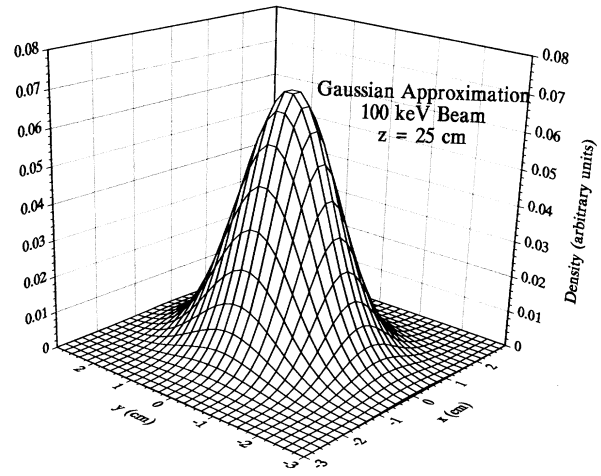

FIG. 13. Three-dimensional Gaussian approximation to the density profile of a 100-keV beam 25 cm from the emission aperture. Compare to Fig. 6.

and a width of 0.5 cm for a 3:1 aspect ratio. In the plane $z=0$, the density is energy independent; so Fig. 3 applies to all beams emerging from extraction systems with this geometry. The corresponding potential appears in Figs. 4 and 14.

Figures 5 and 6 illustrate the evolution of a 100-keV beam as it progresses towards the beam line. At 10 cm, the profile still presents a recognizable aspect ratio, but the cross-sectional dimensions of the beam have increased nearly fourfold. At 25 cm, the beam has assumed a highly symmetric profile, and all traces of the original 3:1 aspect ratio have disappeared.

The tendency of a beam to relax into a particular shape is quite strong. In fact, the initial aspect ratio appears to have little effect on the beam's ultimate configuration. After traveling 25 cm, the topology of the density surface

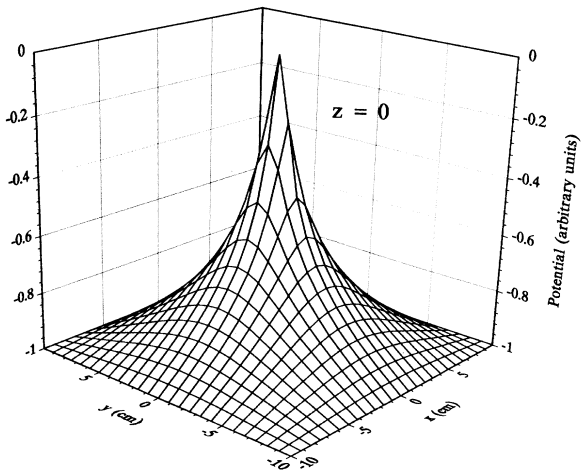

FIG. 14. Potential of a 1.5×0.5 cm^2 beam of arbitrary energy as it emerges from the aperture. Although the beam is rectangular, the resulting potential is remarkably symmetric.

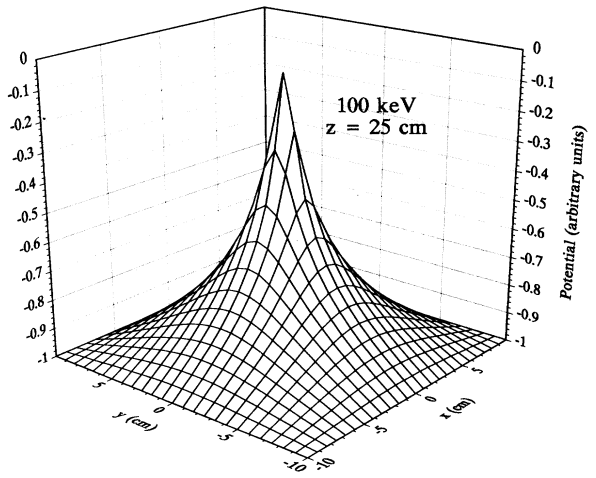

FIG. 15. Potential at $z=25$ cm for a 100-keV beam emitted from a 1.5×0.5 cm^2 aperture.

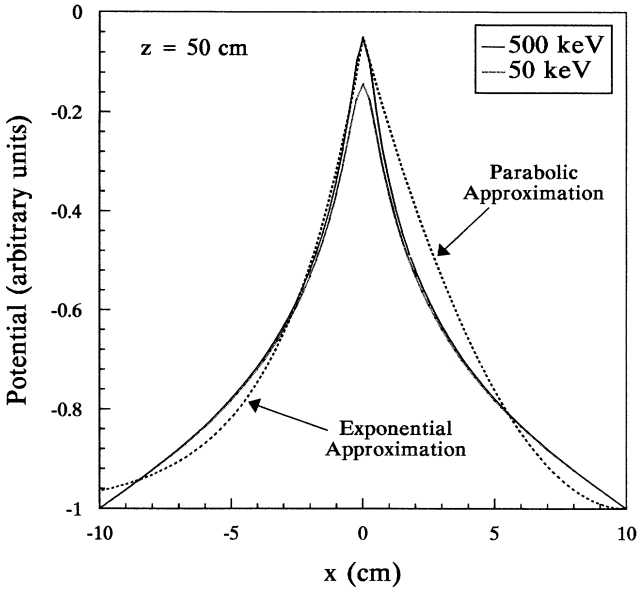

FIG. 16. For 50- and 500-keV beams, at points between half maximum, the potential is well approximated by an exponential function, but is not well described by a quadratic relation.

for an initially thin beam, Fig. 7, is essentially identical to that of an initially square beam, Fig. 8. Potential surfaces for these two cases are displayed in Figs. 9 and 10.

Calculating cross sections along the x axis (Figs. 11 and 12) suggests that between the points of half maximum, the density profile is very well approximated by a Gaussian curve, with the Gaussian decaying much faster near the edges than the curve calculated from Eq. (22). Comparison of the three-dimensional Gaussian plot in Fig. 13 to the predicted surface in Fig. 6 illustrates the high degree to which the beam may be expected to approach the Gaussian shape.

Potentials arising from the above charge distributions are also highly symmetric. The potential of the 1.5 cm$\times$0.5 cm beam at $z=0$ is shown in Fig. 14. Despite the well-defined rectangular shape of the beam in this plane, the potential displays a remarkable degree of cylindrical symmetry. Moreover, although slightly diminished in magnitude, the potential at $z=25$ cm, Fig. 15, differs insignificantly from the $z=0$ surface. As indicated in Fig. 16, the curvature of the potential is well fit by an exponential function, but is not well approximated by a parabolic curve.

IX. CONCLUSION

For beams with axial ion densities, $n_{b0}\gtrsim 10^{12}$ m^{-3} space-charge effects become important. If the beam is collisionless, conservation relations for mass, energy, and phase-space density can be combined with Poisson's equation to obtain an analytic three-dimensional expression describing the beam ion density and the potential of the ensemble. Applying these relations to 50-, 100-, and 500-keV beams, it is concluded that intense beams of all energies and currents ultimately relax into symmetric, near-Gaussian profiles. This is consistent with the assumptions in previous work [4–7]. Moreover, the highly symmetric charge densities give rise to symmetric potential and electric fields in accordance with experimental observations [3].

[1] D. Brown, P. Sferlazzo, and J. O'Hanlon, Nucl. Instrum. Methods Phys. Res. Sect. B **55**, 348 (1991).
[2] D. Brown, P. Sferlazzo, and J. O'Hanlon, J. Am. Vacuum Soc. A **9**, 2808 (1991).
[3] D. Brown, P. Sferlazzo, S. Beck, and J. O'Hanlon, J. Appl. Phys. **71**, 2937 (1992).
[4] A. J. T. Holmes, Phys. Rev. A **19**, 389 (1979).
[5] C. C. Cutler and M. E. Hines, Proc. IRE, 307 (1955).
[6] P. T. Kirstein, IEEE Trans. Electron Dev. **1**, 69 (1963).
[7] P. T. Kirstein, J. Appl. Phys. **34**, 3479 (1963).
[8] Earle H. Kennard, *Kinetic Theory of Gases* (McGraw-Hill, New York, 1938).